

# Structural Design and Analysis of Wind Turbine Tower Cleaning Robot

Lixin SUN<sup>1</sup>, Qi WANG, Chong CHEN and Minglu ZHANG

*School of Mechanical Engineering, Hebei University of Technology, Tianjin300401, China*

**Abstract.** Aiming at the problems of wind turbine tower oil cleaning difficulty and low efficiency of manual operation, design a new wind turbine tower cleaning robot that can replace manual work, reducing labor costs and accident risk. The structural elements and operating principles of the cleaning robot are covered in great detail in this study. To determine the size of the necessary magnetic adsorption force, a hydrostatic study is performed while the robot is in various crawling positions. Maxwell was used to study and simulate the adsorption of the permanent magnet. The simulation findings meet the necessary magnetic adsorption force after the impact of various spacings on the force is examined. The performance of the robot is evaluated after it has undergone physical processing. The results of the studies demonstrate the robot's consistent mobile performance, certain load and obstacle-crossing capability, and effective cleaning capability.

**Keywords.** Wall-Climbing Cleaning Robot; Magnetic simulation; Experiment.

## 1. Introduction

The wind energy sector in China is expanding quickly, and wind energy is being used increasingly frequently in locations with large surfaces. The wind turbine tower's primary function is to support the impeller and act as a shock absorber for the impeller. However, after years of operation, the tower will develop oil stains on its surface, and these stains must be removed[1]. The primary method of cleaning wind turbine towers at the moment is by hand, but this has a number of drawbacks, including its inherently low efficiency and high cost. As a result, it is currently urgently necessary to use robots to complete wind turbine tower cleaning operations rather than by hand[2][3].

At present, the main research contents of wall-crawling cleaning robots are the adsorption method, traveling mechanism, load capacity, and so on[4][5], a suitable travelling mechanism and stable adsorption function are prerequisites for the robot to accomplish its work. There are many wall-climbing robots made specifically for cleaning towers. For instance, the robot made by Xu Chun[6] et al, permanently joins the front drive wheels to the car's body, and there is a gap between the permanent magnets and cylinder wall, which lessens the effectiveness of the magnetic circuit. The robot adopts a four-wheeled mobile mechanism, which increases the robot's dead weight. Its front end is cleaned with a disk brush, which has strong brushing ability at the edges, but the cleaning effect at the center of the circle is poor, and the cleaning effect is not consistent;

---

<sup>1</sup> Corresponding Author, Lixin SUN, School of Mechanical Engineering, Hebei University of Technology, Tianjin 300401, China; E-mail:x211481@163.com.

The tower cleaning robot designed by Hao Yuejiao[7] et al. adopts an electromagnetic adsorption six-legged structure, and the front end also adopts the disk brush cleaning method, electromagnetic adsorption is easy to fall off in case of power failure, the load capacity is low, and the slow movement reduces the cleaning efficiency; Liu Feng[8] et al.'s robot uses a tracked mobile mechanism, and the tracked movement's flexibility is comparatively poor, and the program has excellent safety performance but low moving speed, the front end is cleaned by a roller brush, the cleaning effect is consistent, but the cleaning effect is not so good on the wall with more serious oil stains.

Based on the above problems, this paper designs a wheeled wall-crawling cleaning robot with self-adaptable barrel wall curvature. The adaptive permanent magnet drive wheel movement structure is designed to increase magnetic efficiency. In response to the need for cleaning oil on the cylinder wall, a cleaning mechanism with replaceable wiping cloths has been designed to improve cleaning efficiency. Under various destabilization situations, the static force analysis of the robot was performed, and the theoretical value of the minimum adsorption force was derived. Magnetic simulation result shows that the wheel-type adsorption unit can provide reliable adsorption force. Conduct performance tests on the entire machine to confirm that the robot has excellent mobility, load-bearing capacity and cleaning effect.

## 2. Structural Design of Wind Turbine Tower Cleaning Robot

### 2.1. Robot Overall Structure

The structure of the designed robot is shown in figure 1. The overall structure of the robot adopts a modular design, which is mainly composed of the robot body, permanent magnet drive wheels, and front-end cleaning mechanism. The drive wheels are integrated with the permanent magnets, and the permanent magnet drive wheels provide the main adsorption force for the robot. At the end of the body is a gimbal module with built-in permanent magnets. The gimbal module moves with the body, providing part of the adsorption force and stabilizing support for the body. Cameras are used to monitor the real-time status of the cleaning operation. Synthesizing the production requirements of the robot, the performance indicators that the wall-climbing robot can achieve are shown in table 1.

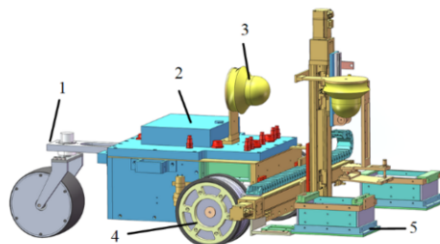


**Figure 1.** Structure of a wind turbine tower cleaning robot (1. gimbal, 2. robot body, 3. camera, 4. permanent magnet drive wheels, 5. cleaning mechanism)

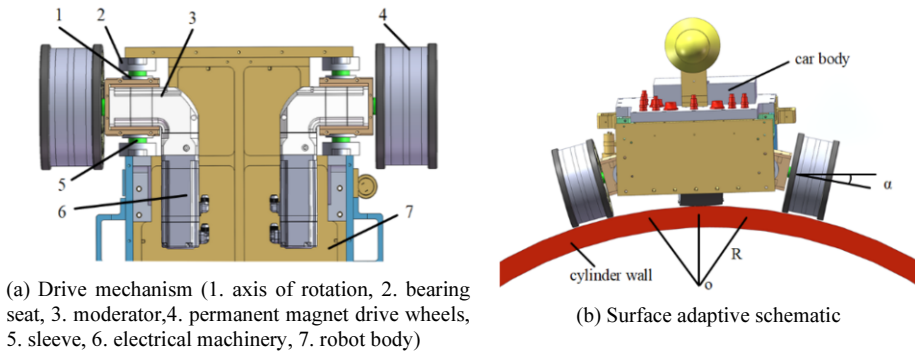
**Table 1.** Cleaning robot technical specifications

Robot parameters	Value
Sizes	1110×898×660 mm
Total robot weight	60 kg
Leapfrogging ability	7 mm
load capacity	53.2 kg

### 2.2. Adaptive Permanent Magnet Drive Wheel Mobile Structure Design

Currently, most wind turbine towers are tapered cylinders, and the curvature of the tower changes with the radius, leading to constant changes in the gap between the permanent magnet wheel and the wall, resulting in the failure of the permanent magnet drive wheel to provide safe and reliable adsorption force, which makes the wall-climbing robots in danger of tipping over. According to the above situation, to design a self-adaptive permanent magnet drive wheel mobile structure, combine the structure of the motor, reducer, and permanent magnet drive wheel fixed connection into one, as shown in figure 2(a).

By increasing the rotational freedom of the permanent magnet drive wheels, the adaptive permanent magnet drive wheel mobile structure has a bit of room for adjustment compared to the fully rigid structure. When the robot touches the wall of the cylinder, the structure rotates around the car body on its axis by magnetic adsorption force. As shown in figure 2(b),  $\alpha$  is increased from zero degree until the end of the close fit of the permanent magnet drive wheel with the wall surface, ensure sufficient adsorption force between the wall-climbing robot and the cylinder wall so that the robot has good adaptability to the radius of curvature of the wind tower.

**Figure 2.** Adaptive permanent magnet drive wheel mobile structure.

### 2.3 Cleaning Mechanism Design

In order to realize the cleaning efficiency of the cleaning robot and not leave stains after cleaning, a cleaning mechanism with replaceable wiping cloths was designed, as shown in figure 3(a). The dirty cloth box and the new cloth box are fixed, the slider on the two

directional modules drives the sticking mechanism and the cloth to move up and down and left and right at the same time, and the sticking mechanism and the cloth can be pulled up from the new cloth box after sticking, and then the cloth is driven to scrub left and right on the cylinder wall until the cloth is dirty, and then it is put into the dirty cloth box, The cleaning mechanism is repeating the process of taking a new step, scrubbing, and placing a dirty cloth.

The cloth sticking mechanism is shown in figure 3(b), and the felt strip on the felt strip mounting plate can be attached to the wiping cloth. A spring is used to pull up the felt strip mounting plate to the limit lever, the limit switch and the limit screw limit the angle of rotation of the felt strip around the rotating axis. In order to avoid excessive wall reaction forces on the fabric cloth sticking mechanism, when the sensor detects the slider on the guide rail, the vertical module pauses to direct the wipe cloth in the direction of the cylinder wall. When the felt strip is detached from the dirty cloth, a large bonding force results if the two contact surfaces of the felt strip and the dirty cloth are separated as a whole, so the felt strip mounting plate is designed to rotate around the rotating axis. during the continuous upward movement of the felt strip, the felt strip will gradually detach from the cloth from the side of the rotating axis until the two contacting surfaces are completely separated, which will greatly reduce the bonding force between the felt strip and the dirty cloth.

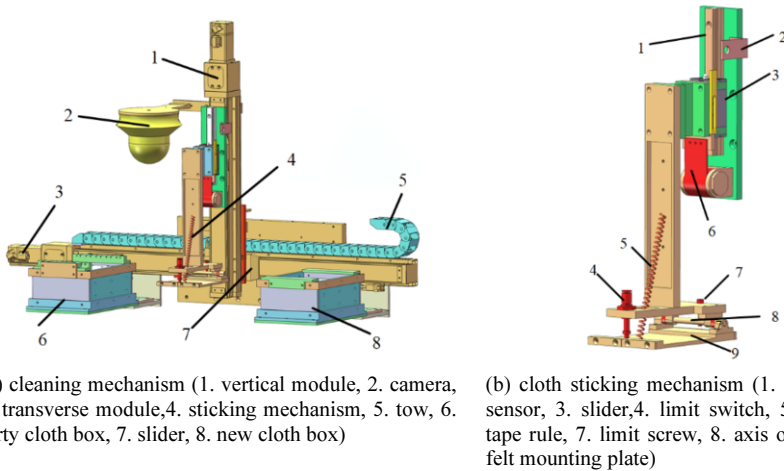


**Figure 3.** Schematic diagram of cleaning mechanism and cloth gluing mechanism.

The principle of the dirty cloth box is shown in figure 4, the sticking mechanism puts the dirty cloth into the box by squeezing the floating plate, the dirty cloth is pressed by the spring between the floating plate and the pressing plate, and the needle is used to fix the dirty cloth to prevent it from being pulled up again by the sticking mechanism. In order to reduce the resistance of up and down movement of the floating plate, the floating plate is designed with steel ball rows on both sides to change the sliding friction into rolling friction, The principle of the new cloth box mechanism is the same as this.

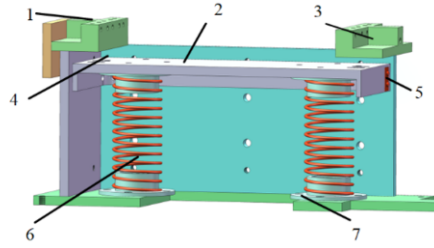


**Figure 4.** Schematic diagram of dirty cloth box (1. needle, 2. floating plate, 3. pressing plate, 4. dirty cloth, 5. steel ball rows, 6. spring, 7. Spring Retainer)

### 3. Adsorption Stability Analysis of Wall-Climbing Robots

This section focuses on the adsorption stability of wall-climbing robots, so the robot needs to be analyzed statically. The robot will experience downward sliding, longitudinal tilting, and transverse overturning as a result of its own weight and the cleaning mechanism's reaction force when it is in use[9]-[10]

#### 3.1. Slide Down Static Analysis

When the motor is energized in the self-locking state, the permanent magnet drive wheel will not rotate, if the wall upward static friction cannot overcome the robot's self-weight, the robot will occur along the wall of the phenomenon of vertical decline, the robot for the static analysis, as shown in figure 5(a).  $F_{mag}$  is the magnetic adsorption force of a single drive wheel on the wall,  $F_m$  is the magnetic adsorption force of a driven universal wheel,  $F_t$  is the reaction force of the wall on the sticking mechanism,  $F_{N1}$  and  $F_{N2}$  are the support forces of a single drive wheel and a universal wheel in contact with the wall, respectively,  $F_{f1}$ ,  $F_{f2}$ , and  $F_{f3}$  are the maximum static friction between a single drive wheel, a universal wheel, a cloth sticking mechanism, and the wall, respectively,  $G$  is the weight of the robot and its load,  $h$  is the perpendicular distance between the center of gravity of the vehicle body and the wall,  $l_1$  is the center spacing of the cloth sticking mechanism and the universal wheel, and  $l_2$  is the center spacing of the drive wheels and universal wheel.

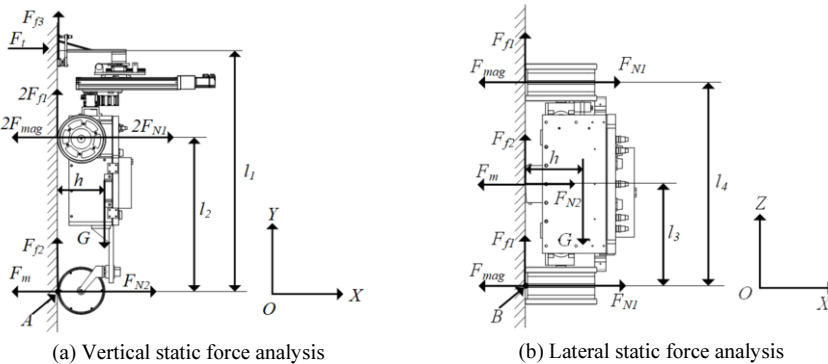


**Figure 5.** Schematic diagram of dirty cloth box.

Universal wheel adsorption force is small, in order to protect safety, the main consideration of the main driving wheel and the wall generated by the static friction is greater than the overall own gravity, the robot does not experience vertical sliding, which needs to satisfy formula (1).

$$\begin{cases} 2F_{f1} \geq G \\ F_{f1} = \mu F_{N1} \\ 2F_{Mag} + F_m = 2F_{N1} + F_{N2} + F_t \\ F_m = F_{N2} \end{cases} \quad (1)$$

where  $\mu$  is the coefficient of friction between the drive wheel and the wall, which can be calculated from formula (1):

$$F_{Mag} > \frac{G}{2\mu} + \frac{F_t}{2} \quad (2)$$

### 3.2. Vertical Rollover Static Analysis

As shown in Fig 5(b), if the moment generated by the magnetic adsorption force is not sufficient to resist the tipping moment generated by gravity, it will cause the car to flip clockwise around point A, taking the torque at point A yields formula (3).

$$\begin{cases} 2F_{Mag}l_2 - 2F_{N1}l_2 - F_t l_1 - Gh > 0 \\ F_{N1} > 0 \\ F_{N2} > 0 \end{cases} \quad (3)$$

From formula (3), the single drive wheel adsorption force requirement can be obtained:

$$F_{Mag} > \frac{F_t l_1 + Gh}{2l_2} \quad (4)$$

### 3.3. Transverse Rollover Static Analysis

The lateral movement of the vehicle body will not carry out the cylinder wall cleaning operation. As shown in figure 5(b) shows the robot lateral state static analysis,  $l_3$  is the distance between the center width of the driving wheel and the universal wheel,  $l_4$  is the distance between the center points of the two driving wheels. In this case, the robot has the risk of overturning around point B, taking the torque at point A yields formula (5).

$$\begin{cases} F_{Mag}l_4 - F_{N1}l_4 + F_m l_3 - F_{N2}l_3 - Gh > 0 \\ F_{N1} > 0 \\ F_{N2} > 0 \end{cases} \quad (5)$$

From formula (3), the single drive wheel adsorption force requirement can be obtained:

$$F_{Mag} > \frac{Gh - F_m l_3}{l_4} \quad (6)$$

The calculations are optimized for walking stability:

$$F_{Mag} > \frac{Gh}{l_4} \quad (7)$$

### 3.4. Calculation of Stationary Instability Extremes

Based on the above analysis of several robot states, the value of the minimum adsorption force required in each case is determined, and taking into account the safety factor  $K$ , the required adsorption force for the robot is:

$$F_{Mag} \geq K \cdot \max \left\{ \frac{G}{2\mu} + \frac{F_t}{2}, \frac{F_t l_1 + Gh}{2l_2}, \frac{Gh}{l_4} \right\} \quad (8)$$

According to the 3D model of the robot:  $l_1=950$  mm,  $l_2=600$  mm,  $l_3=273$  mm,  $l_4=2l_3=546$  mm,  $h=120$  mm,  $K=1.7$ ,  $G=600$  N,  $\mu=0.5$ .

If the size of the reaction force on the wall to the sticking mechanism is 100 N,  $F_t=100$  N, substitute the data into formula (8), the magnetic adsorption force of each permanent magnet wheel must be at least 1 105 N.

## 4. Simulation of the Magnetic Adsorption Mechanism

The contact area between the wheel structure and the wall is small, relative to other mobile institutions, the adsorption force is significantly reduced, so it is necessary to simulate the adsorption structure to verify whether it meets the adsorption force requirements. Robot drive permanent magnet wheel adsorption force is much larger than the universal wheel, and the results of various static analyses are mainly required for the permanent magnet wheel adsorption force, so this paper mainly discusses the design of the magnetic circuit of the permanent magnet drive wheel.

### 4.1. Geometric Model Of Adsorption Mechanism

The permanent magnet adsorption mechanism is shown in figure 6. The magnetic circuit adopts the symmetrical way of axial reversal[11], and the magnetically conductive material is selected between the two axially arranged permanent magnets, the middle area is a magnetic separation material that separates the magnetic lines of the upper and lower permanent magnets, rubber skin avoids collision damage between the permanent magnet and the wall.

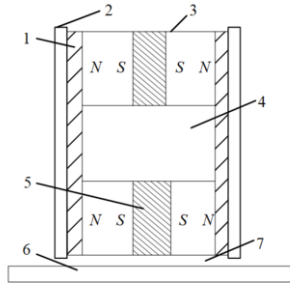


**Figure 6.** Magnetic circuit principle of permanent magnet (1. yoke iron, 2. rubber skin, 3. permanent magnet, 4. magnetic separation material, 5. magnetically conductive material, 6. wall, 7. working gap)

4.2. Modeling and Simulation of Permanent Magnets

Permanent magnet material is N50 with excellent performance[12]. the middle spacing magnetic material is chosen as an aluminum alloy, and the magnetic conductivity and wall material are both adjusted to Q235. Comprehensive robot adsorption force requirements and the quality of the permanent magnet wheel, the overall size of the permanent magnet drive wheel should not be too large, parameterization of the permanent magnet drive wheel structure according to the above requirements. The permanent magnet has an outer diameter of 180 mm, an inner diameter of 120 mm, and a width of 20 mm. The magnet guide and yoke have the same inner and outer dimensions as the permanent magnet, the magnet conductor has a width of 22 mm, and the yoke has a width of 10 mm. the magnetically conductive wall is 340 mm long, 200 mm wide, and 10 mm thick. the gap between the permanent magnet and the wall is 5 mm, the material in the gap is air, and the relative permeability is set to 1.

The permanent magnet is simulated in Maxwell 2D, and the result of magnetic lines of force is shown in figure 7(a), the magnetic lines of force are emitted from the inside of the permanent magnet, guided by the yoke through the working wall, and finally returned to the permanent magnet by the permeable material to form a closed loop. the area between the permanent magnet wheel and the wall is a dense area of magnetic lines of force, where the magnetic force is at its maximum. The magnetic induction strength is measured on the permanent magnet, and the simulation results are shown in figure 7(b).

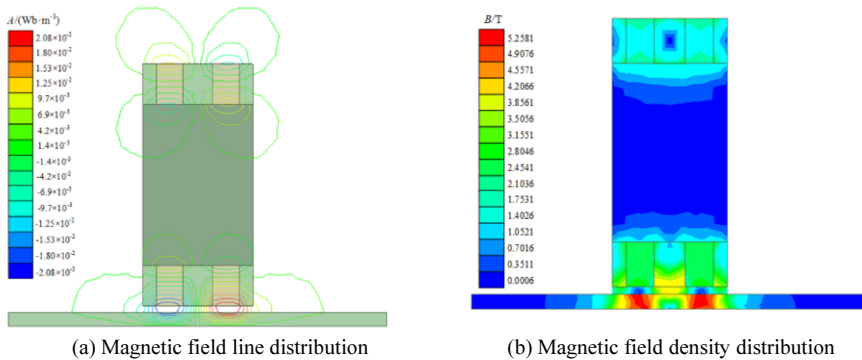


**Figure 7.** Permanent magnet simulation results.

A permanent magnet drive wheel across the weld will exist a distance from the wall, resulting in a sharp decline in the adsorption force, resulting in the robot instability phenomenon, so it is necessary to analyze the change rule of the permanent magnet wheel adsorption force with the wall gap. The variable range of the permanent magnet gap  $d$  from the wall is 0~10 mm, and the curve of the magnetic adsorption force versus the gap  $d$  is simulated in Maxwell 3D, which is shown in figure 8, and the magnetic adsorption force decreases sharply with the increase of the gap. When the gap between the permanent magnet and the wall is 8 mm, the simulation result of the adsorption force is 1120 N. As shown in formula (8), the theoretical adsorption force that each permanent magnet driving wheel provides is at least 1105 N, and the simulation result is greater than the calculated theoretical adsorption force, considering that the outer diameter of the rubber skin is larger than that of a permanent magnet by 2 mm, and ignoring the effect of deformation of the rubber skin due to the extrusion by the wall, the rubber skin will enlarge the gap by 1 mm, therefore, in the height of the seam of 0~7 mm, the adsorption force provided by the permanent magnet driving wheel can meet the demand of overcoming the obstacle.

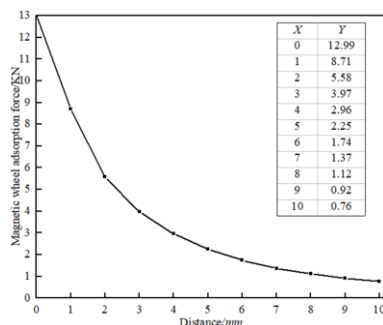


Figure 8. Variation curve of magnetic adsorption force with gap.

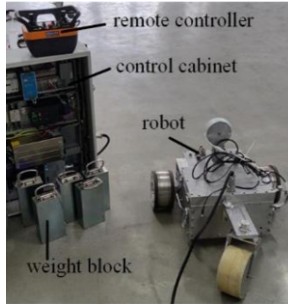
## 5. Robot Performance Test Experiment

Through the structural design and magnetic simulation results, the wall-climbing robot entity is designed and produced, and in order to verify the reasonableness of the above calculations and simulations, the robot is subjected to performance test experiments on the simulation test bench and in the real environment to check the overall function of the robot, respectively.

### 5.1. Weight-bearing and Obstacle-crossing Ability Tests

The test platform was modelled after a real wind turbine tower, with a bottom diameter of 2.5 m and a top diameter of 2 m. The material is Q235 steel with a wall thickness of 8 mm, as shown in figure 9. Weight-bearing tests in longitudinal, lateral, and steering attitudes were performed on this experimental platform. 9(a) is the tool used by the robot to perform the weight-bearing experiment, the control cabinet and the robot are connected by cables so that the robot's movement can be controlled remotely using a remote control. 9(b) shows that the load weight of one piece is 13.3 KG, and the experiment verifies that the robot can withstand up to 4 pieces of loads, so the robot can

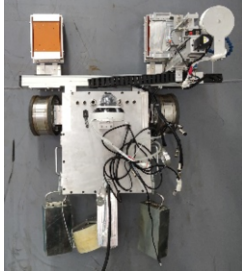
withstand a load weight of 53.2 KG. the load will increase the risk of robot destabilization, but the robot did not destabilize in any of the above cases, and the steering process is flexible in the same place, which proves that the robot has excellent mobility performance. The robot can successfully cross a weld seam in experiment 9(f), which shows that it has some obstacle-crossing capacity. The weld seam height is 6mm.



(a) Experimental tools



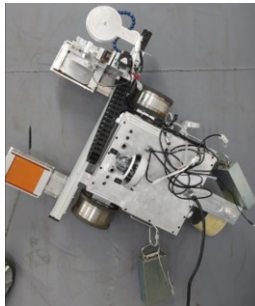
(b) Weight test for load block



(c) Vertical load test



(d) Transverse load test



(e) Steering load test



(f) Cross weld test

**Figure 9.** Weight-bearing and obstacle-crossing ability tests.

## 5.2. Wind Turbine Tower Oil Cleaning Experiment

As shown in figure 10, an oil cleaning test was performed in the real environment in order to verify the efficiency of the robot's operation. The experiments on the robot's mobility are displayed in 10(b), which shows that the robot can realize smooth operation in the real environment, and its mobile speed can reach 10 m/min, which meets the efficiency requirements for the cleaning operation. The oil contamination on

the barrel wall before robotic cleaning is depicted in figure 10(c), and the oil contamination on the wind turbine tower has accumulated significantly and is challenging to entirely remove. After robot cleaning, figure 10(d) shows the oil contamination on the cylinder wall, the experiment shows that the robot's cleaning effectiveness is excellent since, the cylinder wall surface oil is clean and free of spots after cleaning the cylinder wall oil.



(a) wind turbine tower



(b) Mobile performance experiment



(c) Pre-cleaning



(d) Post-cleaning

**Figure 10.** Wall oil cleaning test.

## 6. Conclusion

Aiming at the wind turbine tower oil cleaning difficulties and low efficiency of manual operation, design a new wind turbine tower cleaning robot that can replace manual labor. The permanent magnet drive wheel has rotational freedom to adapt to different curvatures of the wall, to ensure that the robot has enough adsorption force with the cylinder wall. The front-end cleaning mechanism is a replaceable cloth design, which can complete the wind turbine tower wall oil cleaning work.

Combined with the force analysis of the robot, various attitude static analyses were carried out to calculate the size of the required adsorption force, and magnetic simulation was carried out to obtain the variation curve between the adsorption force and the gap, which proved that the adsorption force provided by the permanent magnet drive wheel within the gap of 7 mm can meet the requirement of more than 1105 N, ensuring that the robot will not be in danger of sliding, tipping, or toppling.

According to the robot performance experiments, the robot can run stably on the cylinder wall under full load and complete the functions of crossing obstacles, traveling

straight, steering, etc. The robot has superior mobile performance. Through the wind power tower cleaning experiment, it can be seen that the wall is smooth and neat after cleaning, and the cleaning efficiency is high.

## Acknowledgement

This research work was supported by Bingoo Robot.

## References

- [1] Espinoza R V, Oliveira A S D, Arruda L V R D, et al. Navigation's stabilization system of a magnetic adherence-based climbing robot [J]. *Journal of Intelligent&Robotic Systems*, 2015, 78 (1): 65-81.
- [2] Kakogawa A, Ma S. Speed analysis for three driving modules of an in-pipe inspection robots for passing through bent pipes [C]//*IEEE International Conference on Robotics&Biomimetics*. Piscataway: IEEE, 2015: 1731-1736.
- [3] Lu Z X, Xu C G, Pan Q X, et al. Automatic method for synchronizing workpiece frames in twin-robot nondestructive testing system [J]. *Chinese Journal of Mechanical Engineering*, 2015, 28 (4): 860-868.
- [4] Ma J L, Peng J, Guo Y J, et al. Current status and trend of wall climbing research [J]. *Journal of Mechanical Engineering*, 2023, 59 (05): 11-28.
- [5] Li L, Yang X, Qin X J, et al. Current status and development trend of wall-crawling and washing robots [J]. *Mechanical Manufacturing and Automation*, 2023, 52 (01): 1-6.
- [6] Xu C, Liu H D, Zhao Z F, et al. Design of a robotic system for oil cleaning and non-destructive testing of wind turbine towers [J]. *Equipment management and maintenance*, 2022, (14): 50-53.
- [7] Hao Y J. Structural design and analysis of a wind turbine tower cleaning robot. [D]. Lanzhou University of Science and Technology, 2019.
- [8] Liu F. Design and Research of Wind Turbine Tower Cleaning Robot. [D]. Harbin Institute of Technology, 2013.
- [9] Cai J, He K, Fang H, et al. The design of permanent-magnetic wheeled wall-climbing robot [C]//*IEEE International Conference on Information and Automation*, New York: IEEE, 2017: 604-608.
- [10] Huang H, Li D, Xue Z, et al. Design and performance analysis of a tracked wall-climbing robot for ship inspection in shipbuilding [J]. *Ocean Engineering*, 2017, 131: 224-230.
- [11] Xue S, Feng Z Q, Xu L, et al. An ANSYS-based-based of a permanent magnet adsorption unit for wall-climbing robots [J]. *Manufacturing Automation*, 2016,38 (8):22-25.
- [12] Gao H, Feng Y G, et al. The latest application progress of permanent magnet materials and their prospect analysis [J]. *Energy and Environmental Protection*, 2019,41 (1):89-92.